



UNIVERSITI PUTRA MALAYSIA

**DEVELOPMENT AND APPLICATIONS OF PHOTOFLASH-PVDF
TECHNIQUE IN THERMAL DIFFUSIVITY MEASUREMENT AT LOW
TEMPERATURES**

MEHDI HAYDARI.

FSAS 2004 12

**DEVELOPMENT AND APPLICATIONS OF PHOTOFLASH-PVDF
TECHNIQUE IN THERMAL DIFFUSIVITY MEASUREMENT AT LOW
TEMPERATURES**

By

MEHDI HAYDARI

**Thesis Submitted to the School of Graduate Studies, Universiti Putra Malaysia,
in Fulfilment of the Requirement for the Degree of Doctor of Philosophy**

May 2004



DEDICATION

To my beloved parents

Hossein Haydari & Leila Nikbakht

They are the first and the best in my life

and

**My supervisor Professor Dr. Mohd Maarof H. A. Moxin
for his guidance, advice and endless supports**

Abstract of thesis presented to the Senate of Universiti Putra Malaysia in
Fulfilment of the requirement for the degree of Doctor of Philosophy

**DEVELOPMENT AND APPLICATIONS OF PHOTOFLASH-PVDF
TECHNIQUE IN THERMAL DIFFUSIVITY MEASUREMENT AT LOW
TEMPERATURES**

By

MEHDI HAYDARI

May 2004

Chairman: Professor Mohd Maarof H. A. Maksin, Ph. D.

Faculty: Science and Environmental Studies

The photoflash technique is developed and used for measuring thermal diffusivity of various types of material, at temperature range from $\sim 77\text{K}$ to ambient temperature. It uses a cheap and simple camera flash and polyvinylidene difluoride (PVDF) film as signal generating source and detector, respectively.

The theoretical signal was derived based on the square pulse approximation of the camera flash that replaced Dirac- δ function approximation employed in other studies. Comparative studies on these two different approximations have been performed on SiC/B₄C composites. Although the camera flash temporal shape is closer to square pulse, Dirac- δ function approximation is still valid for the limited

case of PVDF signal that is significantly longer than camera flash pulse duration.

The square wave approximation model was further used in determining the thermal diffusivity of superconductors, semiconductors, magnetoresistances, carbon nanotubes, ceramics, composites, polymers and porous samples.

The thermal diffusivity for SiC/B₄C composites and SiC doped with Al decreased with increasing temperature. This suggests that thermal diffusivity is basically influenced by phonon interaction within lattice that determines the phonon mean free path.

In case of superconducting materials, thermal diffusivity measurements were carried for BSCCO, doped with Samarium (Sm) at Bi, Sr and Cu sites and sintered for 24, 48 and 100hrs respectively. The results were explained in terms of electron-phonon and phonon-lattice interactions in association with the sample grain size.

The magneto-resistive of LCMO doped with Er at La site was also studied in this study. Thermal diffusivity measurements revealed that the transition from metallic to insulator and from insulator to semiconductor behavior in the materials, were closely matched to the results obtained from electrical resistivity measurement of other researchers.

The thermal diffusivity of carbon nanotubes (CNTs) decreased when the temperature was increased from low to room temperature. Besides, there were also

double slope phenomena in the way the thermal diffusivity changed with composition of CNT in the range of temperature covered in the measurement.

In the case of polymers of Emeraldine Base (EB) and Emeraldine Salt (ES), the thermal diffusivity changed with temperature as in other insulating materials.

Finally, the effect of porosity on thermal diffusivity was studied using Nickel Copper Zinc Ferrite samples. The thermal diffusivity decreased with increasing porosity of the sample. The results also showed that porosity has a greater effect on thermal conductivity of the material than its thermal capacity.

Abstrak tesis yang dikemukakan kepada Senat Universiti Putra Malaysia sebagai memenuhi keperluan untuk ijazah Doktor Falsafah

**PEMBANGUNAN DAN PENGGUNAAN TEKNIK FOTOKILAT-PVDF
DALAM PENGUKURAN PERESAPAN TERMA PADA SUHU-SUHU
RENDAH**

Oleh

MEHDI HAYDARI

Mei. 2004

Pengerusi: Profesor Mohd Maarof H. A. Moxin, Ph. D.

Fakulti: Sains dan Pengajian Alam Sekitar

Teknik fotokilat telah dibangunkan dan digunakan untuk mengukur resapan terma yang mempunyai bidang yang lebar daripada suhu rendah $\sim 77\text{K}$ kepada suhu ambien untuk pelbagai jenis bahan. Ia menggunakan 'camera flash' dan filem polyvinilidene difluoride (PVDF) yang murah dan sederhana, masing-masing sebagai sumber penjana dan pengesan isyarat.

Isyarat teori telah diterbitkan berdasarkan penghampiran kepada denyut segi empat untuk camera flash menggantikan penghampiran fungsi Dirac- δ yang biasa digunakan dalam kerja-kerja sebelum ini. Kajian perbandingan bagi kedua-dua penghampiran ini telah dijalankan ke atas beberapa sampel komposit SiC/B₄C. Walaupun bentuk tempohan daripada camera flash lebih hampir kepada bentuk denyut segi empat, namun penghampiran fungsi Dirac- δ masih sah digunakan

untuk kes yang terhad kepada isyarat PVDF yang jauh lebih panjang berbanding dengan tempoh denyut kilat camera flash dalam kejian ini.

Model penghampiran bagi gelombang segi empat adalah seterusnya digunakan untuk menentukan pemalar peresapan terma bagi bahan superkonduktor, semikonduktor, magnetoresistan, nanotiub karbon, seramik, polimer dan bahan berliang.

Hasil yang diperolehi untuk komposit SiC/B₄C dan SiC yang didop dengan Al menunjukkan peresapan terma mengecil dengan kenaikan suhu yang mana memberi petunjuk yang resapan terma pada asasnya dipengaruhi oleh saling tindak antara fonon dengan kekisi yang akan menentukan lintasan bebas min untuk fonon.

Dalam hal bahan superkonduktor, pengukuran resapan terma telah dilakukan ke atas BSCCO yang didop dengan Samarium (Sm) pada tapak Bi, Sr dan Cu yang masing-masing disinter selama 24, 48 dan 100 jam. Hasil yang diperolehi dihuraikan dari aspek saling tindak lektron-fonon dan fonon-kekisi yang ada kaitannya dengan dengan saiz butir sample.

Sampel magneto-resistif bagi LCMO yang didop dengan Er pada tapak La telah juga dikaji. Hasil pengukuran resapan terma yang diperolehi telah menyerlahkan gelagat peralihan dari logam ke penebat dan dari penebat ke semikonduktor dalam bahan, hamper sama dengan yang diperolehi dari hasil pengukuran rintangan elektrik yang dilakukan oleh orang lain.

Sampel karbon nanotub (CNT) menunjukkan resapan terma dari suhu rendah ke suhu bilik adalah mengecil dengan kenaikan suhu sebagaimana yang berlaku pada bahan penebat yang lain. Disamping itu terdapat fenomena dua cerun bagaimana resapan terma berubah dengan komposisi CNT pada bidang suhu yang diliputi dalam pengukuran ini.

Dalam hal polimer Emeraldine Base (EB) dan Emeraldine Salt (ES), resapan terma berubah dengan suhu sebagaimana dalam bahan penebat yang lain.

Akhir sekali, kesan liang pada resapan terma telah dikaji dengan menggunakan sampel Nickel Copper Zinc Ferrite. Resapan termanya menurun dengan kenaikan keliangan sampel. Hasil pengukuran juga menunjukkan keliangan memberi kesan yang lebih besar kepada konduktiviti terma bahan dibandingkan dengan kapasiti termanya.

ACKNOWLEDGEMENTS

I would like to express my sincere gratitude to my supervisor, Professor Dr. Mohd Maarof H. A. Moksini for his guidance and advice during this research. His encouragement, moral and technical support made this work possible.

I am also grateful to my supervisory committee, Professor Dr. W. Mahmood Mat Yunus, Professor Dr. Abdul Halim Shaari and Associate Professor Dr. Ionel Valeriu Grozescu for their advice and helpful discussion during this period of study.

The best appreciation to Ir. Mohammad Ali Heidari, Dr. Hamid Assilzadeh and Dr. Javad Sameni who have helped and supported me from the first day of my stay in Malaysia.

Special thanks are also due to Associate Professor Dr. Zaidan Abd. Wahab and Associate Professor Dr. Azmi bin Zakaria for the useful discussions during the experiments and for providing some of the samples used in this work and the use of the facilities at their laboratories.

I would like to thank:

- Dr.Imad Hamadneh and Dr.Noorhana Yahya for providing the samples.
- All the staff in physics department, UPM for their co-operation given to me throughout my work.
- Physics Department in particular and Universiti Putra Malaysia in general for research supports through IRPA and Graduate Research Assistantship.
- All the Malaysian people especially UPM staff for the best hospitalities.
- All of Iranian and overseas students who involved directly or indirectly towards the success of this project.

Finally, I wish to acknowledge the support from my parents throughout my study from the beginning of my education.

I certify that an Examination Committee met on 28th May 2004 to conduct the final examination of Mehdi Haydari on his Doctor of Philosophy thesis entitled “Development and Applications of Photoflash-PVDF Technique in Thermal Diffusivity Measurement at Low Temperatures” in accordance with Universiti Pertanian Malaysia (Higher Degree) Act 1980 and Universiti Pertanian Malaysia (Higher Degree) Regulations 1981. The Committee recommends that the candidate be awarded the relevant degree. Members of the Examination Committee are as follows:

KAIDA BIN KHALID, Ph.D.

Professor
Faculty of Science and Environmental Studies
Universiti Putra Malaysia
(Chairman)

ZAIDAN ABD WAHAB, Ph.D.

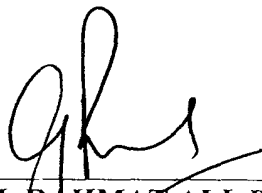
Associate Professor
Faculty of Science and Environmental Studies
Universiti Putra Malaysia
(Member)

AZMI BIN ZAKARIA, Ph.D.

Associate Professor
Faculty of Science and Environmental Studies
Universiti Putra Malaysia
(Member)

MUHAMAD MAT SALLEH, Ph.D.

Professor
Faculty of Science and Technology
Universiti Kebangsaan Malaysia
(Independent Examiner)



GULAM RUSUL RAHMAT ALI, Ph.D.

Professor/Deputy Dean
School of Graduate Studies
Universiti Putra Malaysia

Date:

27/7/04.

This thesis submitted to the Senate of Universiti Putra Malaysia and has been accepted as fulfilment of the requirements for the degree of Doctor of Philosophy. The members of the Supervisory Committee are as follows:

MOHD MAAROF MOKSIN, Ph.D.

Professor
Faculty of Science and Environmental Studies
Universiti Putra Malaysia
(Chairman)

W. MAHMOOD MAT YUNUS, Ph.D.

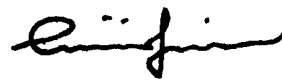
Professor
Faculty of Science and Environmental Studies
Universiti Putra Malaysia
(Member)

ABDUL HALIM SHAARI, Ph.D.

Professor
Faculty of Science and Environmental Studies
Universiti Putra Malaysia
(Member)

IONEL VALERIU GROZESCU, Ph.D.

Associate Professor
Faculty of Science and Environmental Studies
Universiti Putra Malaysia
(Member)



AINI IDERIS, Ph.D.

Professor/Deputy Dean
School of Graduate Studies
Universiti Putra Malaysia

Date: 16 AUG 2004

DECLARATION

I hereby declare that the thesis based on my original work except for quotations and citations, which have been duly acknowledged. I also declare that it has not been previously or concurrently submitted for any other degree at UPM or other institutions.



MEHDI HAYDARI

Date: 30, 7, 2004

TABLE OF CONTENTS

	Page
DEDICATION	ii
ABSTRACT	iii
ABSTRAK	vi
ACKNOWLEDGEMENTS	ix
APPROVAL	x
DECLARATION	xii
LIST OF TABLES	xvi
LIST OF FIGURES	xvii
LIST OF ABBREVIATIONS	xxii
LIST OF SYMBOLS	xxiv
CHAPTER	
I INTRODUCTION	1
Photothermal Technique	2
Photoflash Technique	3
Thermal Properties of Materials	5
Objectives	7
II LITERATURE REVIEW	9
Signal Generation Process	10
Light Modulated Method	11
Light Pulsed Method	13
Modulated CW and Pulsed Generated Signal Detection	14
Detection Methods	19
Direct Detection Methods	20
Indirect Detection Methods	21
Photoflash Technique Applications in Thermal Diffusivity	
Measurement	21
Applications of PVDF Sensor in Photoflash Technique	22
Theory of Photoflash Technique	23
Effect of Finite Pulse	25
Effect of Sample Thickness	26
Effect of the Heat Loss	26
Effect of the Sample Properties on Thermal Diffusivity	26
Effect of Sample Temperature on Thermal Diffusivity	27
	xiii

Other Related Work	27
Photoacoustic Technique	28
Thermocouple Detection	29
Photodeflection Technique	30
Photothermal Displacement Technique	31
Optothermal Transient Emission Radiometry Technique	33
Thermal Carriers in Solids	34
Lattice and Electronic Specific Heats	35
Electronic Specific Heat	39
Cooper Pairs	40
The Electron-Lattice Interaction	42
 III THEORY	 46
Pyroelectric Detection	46
Calculation of PVDF Signal as Generated by the Pulse Light	47
Instantaneous Optical Pulse Generated Signal (Dirac- δ)	49
Experimental Conditions and Approximations to the Model	52
Thermal Insulator Backing	53
Metallic Backing ($b_{43} \gg 1$) and Thermally Thick	
Sample ($q_2 l \gg q_3 d$)	54
Metallic Backing ($b_{43} \gg 1$) and Thermally Thin	
Sample ($q_2 l \ll q_3 d$)	55
Square Optical Pulse Generated Signal	56
Thermal Insulator Backing	57
Metallic Backing ($b_{43} \gg 1$) and Thermally Thick	
Sample ($q_2 l \gg q_3 d$)	58
Metallic Backing ($b_{43} \gg 1$) and Thermally Thin	
Sample ($q_2 l \ll q_3 d$)	60
Simulation Results for Square Pulse Theoretical Model	60
The Effect of Backing	61
The Effect of Thermal Conductivity and Diffusivity	62
The Effect of the Pulse Shape	67
 IV METHODOLOGY	 69
Photoflash	69
PVDF	70
Digital Oscilloscope	73
Sample Chamber	74
Other Apparatus	75
Samples Preparation	76

Superconductors	77
Semiconductors	78
Magnet	79
Carbon Nanotubes (CNTs)	80
Polyaniline (EB and ES)	80
Porous Sample	81
Experimental Procedure	82
PVDF Signal	84
Signal Normalization	85
Signal Averaging and Noise Reduction	85
Data Analysis	88
Fitting Procedure in Determining Thermal Diffusivity and Error Estimation	89
 V RESULTS AND DISCUSSION	 92
Optimum Thickness	92
Comparison of Dirac- δ and Square Heating Pulse	95
Hysteresis Effect	99
Superconductors	100
Thermal Diffusivity of Pure BSCCO	101
Thermal Diffusivity of Sm Doped BSCCO at Bi Site	106
Thermal Diffusivity of Sm Doped BSCCO at Sr Site	108
Thermal Diffusivity of Sm Doped BSCCO at Cu Site	115
Semiconductors	120
SiC/B ₄ C Composite	121
Al Doped SiC	122
Magnet	124
Carbon Nanotubes (CNTs)	127
Polyaniline Sample (EB and ES)	130
Porous Sample	132
 VI CONCLUSION AND FUTURE DIRECTIONS	 136
Conclusion	136
Recommendations	138
 REFERENCES	 140
APPENDICES	146
BIODATA OF THE AUTHOR	163

LIST OF TABLES

Table	Page
3.1 Physical properties of the samples at room temperature	64
5.1 Values of thickness, thermal diffusivity and thermal conductivity for respective samples	98
5.2 Thermal diffusivity of Sm doped $\text{Bi}_{1.6-x}\text{Pb}_{0.4}\text{Sr}_{2-x}\text{Ca}_2\text{Cu}_3\text{Sm}_x\text{O}_8$ ($x=0.02-0.4$) Superconductor ceramic in Bi site at 24 hrs sintering time	107
5.3 Thermal diffusivity of Sm doped $\text{Bi}_{1.6}\text{Pb}_{0.4}\text{Sr}_{2-x}\text{Ca}_2\text{Cu}_3\text{Sm}_x\text{O}_8$ ($x=0.02-0.4$) superconductor ceramic in Sr site at 24, 48 and 100 hrs sintering time	110
5.4 Thermal diffusivity of Sm doped $\text{Bi}_{1.6}\text{Pb}_{0.4}\text{Sr}_2\text{Ca}_2\text{Cu}_{3-x}\text{Sm}_x\text{O}_8$ ($x=0.02-0.4$) superconductor ceramic in Cu site at 24, 48 and 100 hrs sintering time	115
5.5 Values of thickness, thermal diffusivity for respective samples	129
5.6 Thermal diffusivity for ferrite samples	133

LIST OF FIGURES

Figure	Page
2.1 Schematic of the photothermal signal generation process	10
2.2 Schematic photothermal signal generation process in a thermally thick sample as a function of absorption length A	17
2.3 Schematic of the photothermal signal generation process in an optically opaque sample as a function of thermal diffusion length D	19
2.4 Photodeflection scheme: normal and lateral components associated to the refractive index gradient in air	30
2.5 Schematic illustration of the photothermal displacement technique	32
2.6 Schematic representation Cooper pair and lattice spacing	40
2.7 Schematic representation Cooper pair attraction	41
2.8 Schematic representation of electron- electron interaction transmitted by a phonon	43
3.1 Schematic diagram of the four-layer system	48
3.2 Theoretical result for gold sample obtained by substituting Eq (3.32) and (3.34) for the case of thermal insulator and metallic sample backing respectively	61
3.3 Backing effect on signal	62
3.4 Effect of the thermal diffusivity (α) on the signal in the case of rubber backing	63
3.5 Effect of the thermal conductivity (k) on the signal in the case of rubber back	64
3.6 Effect of the thermal diffusivity (α) on the signal in the case of metal backing	65
3.7 Effect of the thermal conductivity (k) on the signal in the case of metal back	66

3.8	The effect of the pulse shape	67
4.1	Experimental and theoretical photoflash temporal profile	70
4.2	Cross section of PVDF from two sides view	71
4.3	The rise time of the PVDF	71
4.4	Temperature dependence of α (solid square) and k (hole square) on temperature for PVDF (Bonno et al, 2001) fitted by 4 th order polynomial	72
4.5	Arrangement inside the cooling chamber	75
4.6	Schematic diagram of the experimental setup	82
4.7	Experimental setup	83
4.8	The PVDF response from $\text{Bi}_{1.6}\text{Pb}_{0.4}\text{Sr}_2\text{Ca}_2\text{Cu}_3\text{O}_\delta$ with 100 hrs sintering time at room temperature	84
4.9	PVDF signal from $\text{Bi}_{1.6}\text{Pb}_{0.4}\text{Sr}_2\text{Ca}_2\text{Cu}_3\text{O}_\delta$ with 24 hrs sintering time due to single shot pulsed camera flash	86
4.10	Signal averaging effectiveness on the noise reduction in the signal from $\text{Bi}_{1.6}\text{Pb}_{0.4}\text{Sr}_2\text{Ca}_2\text{Cu}_3\text{O}_\delta$ with 24 hrs sintering time due to shot pulsed camera flash	87
4.11	Typical PVDF response from $\text{Bi}_{1.6}\text{Pb}_{0.4}\text{Sr}_2\text{Ca}_2\text{Cu}_3\text{O}_\delta$ with 100 hrs sintering time at room temperature (square) fitted by theoretical model (solid line)	88
4.12	Graphic user interface of Microcal Origin 6.0 software in defining the fitting equation and parameters with the experimental plot indicated in background	90
4.13	Graphic user interface of Microcal Origin 6.0 software in fitting session with the experimental plot and simulated curve indicated in background	90
5.1	PVDF response from $\text{Bi}_{1.6}\text{Pb}_{0.4}\text{Sr}_2\text{Ca}_2\text{Cu}_3\text{O}_\delta$ with 24 hrs sintering time at room temperature for thick and thin samples respectively	93
5.2	Thermal diffusivity, (α) versus thickness, L for $\text{Bi}_{1.6}\text{Pb}_{0.4}\text{Sr}_2\text{Ca}_2\text{Cu}_3\text{O}_\delta$ with 24 hrs sintering time	93

5.3	Rise time, t_p versus sample thickness, L	94
5.4	PVDF signals from SiC/B ₄ C composites of different % B ₄ C fitted with pulse (Dirac- δ) function heating model	96
5.5	PVDF signals from SiC/B ₄ C composites of different % B ₄ C fitted with square pulse heating model	97
5.6	Comparison between thermal diffusivity obtained from square pulse and Instantaneous pulse (Dirac- δ) heating model	98
5.7	Thermal diffusivity of SiC versus temperature	100
5.8	PVDF response for Bi _{1.6} Pb _{0.4} Sr ₂ Ca ₂ Cu ₃ O ₈ (BSCCO) at 24, 48 and 100 hrs sintering time in 85 and 300K. Similar responses were observed at different temperature. Solid curves correspond to the theoretical model based on the Eq (3.32)	102
5.9	Thermal diffusivity as a function of temperature for pure BSCCO at 24, 48 and 100 hrs sintering time. The abrupt increase in the thermal diffusivity is seen around the transition temperature which is enlarged in the figure on the right	103
5.10	thermal diffusivity as a function of temperature for pure BSCCO at 24, 48 and 100 hrs sintering time	105
5.11	Thermal diffusivity of Bi _{1.6-x} Pb _{0.4} Sr ₂ Ca ₂ Cu ₃ Sm _x O ₈ (x=0.02-0.4) versus composition of Sm doped at Bi site at 24 hrs sintering time as measured by using PVDF and thermocouple respectively at room temperature	106
5.12	Thermal diffusivity as a function of temperature for BSCCO doped with Sm in Bi site at 24hrs sintering time. The abrupt increase in the thermal diffusivity is seen around the transition temperature as shown in the enlarged figure on the right	108
5.13	Thermal diffusivity of Bi _{1.6} Pb _{0.4} Sr _{2-x} Ca ₂ Cu ₃ Sm _x O ₈ (x=0.02-0.4) versusSm composition at Sr site at 24, 48 and 100 hrs sintering time respectively	109
5.14	Thermal diffusivity as a function of temperature for BSCCO doped with Sm (x=0.02) at Sr site for 24, 48 and 100hrs sintering time. The abrupt increase and decrease in the thermal diffusivity is seen around the transition temperature as shown in the enlarged figure on the right	111

5.15	Thermal diffusivity as a function of temperature for BSCCO doped with Sm ($x=0.06$) at Sr site for 24, 48 and 100hrs sintering time respectively	112
5.16	Thermal diffusivity as a function of temperature for BSCCO doped with Sm ($x=0.02$) at Sr site at 24 and 100 hrs sintering time.	114
5.17	Thermal diffusivity as a function of temperature for BSCCO doped with Sm ($x=0.06$) at Sr site at 24, 48 and 100 hrs sintering time	114
5.18	Thermal diffusivity of $\text{Bi}_{1.6}\text{Pb}_{0.4}\text{Sr}_2\text{Ca}_2\text{Cu}_{3-x}\text{Sm}_x\text{O}_8$ ($x=0.02-0.4$) versus composition of Sm at Cu site for 24, 48 and 100 hrs sintering time	116
5.19	Thermal diffusivity as a function of temperature for BSCCO doped with Sm ($x=0.02$) at Cu site for 24 and 100hrs sintering time. The abrupt increase in the thermal diffusivity is seen around the transition temperature	117
5.20	Thermal diffusivity as a function of temperature for BSCCO doped with Sm ($x=0.06$) at Cu site for 24, 48 and 100hrs sintering time. The abrupt increase in the thermal diffusivity is seen around the transition temperature.	118
5.21	Thermal diffusivity as a function of temperature for BSCCO doped with Sm ($x=0.02$) at Cu site at 24 and 100 hrs sintering time.	119
5.22	Thermal diffusivity as a function of temperature for BSCCO doped with Sm ($x=0.06$) at Cu site at 24, 48 and 100 hrs sintering time	120
5.23	Thermal diffusivity versus temperature from 200K to 300K for the respective samples.	122
5.24	Thermal diffusivity versus temperature from 200K to 300K for the respective samples	124
5.25	Thermal wave response from $(\text{La}_{1-x}\text{Er}_x)_{0.67}\text{Ca}_{0.33}\text{MnO}_3$ [$0 \leq x \leq 0.03$] sample at 100K fitted by theoretical model based on Eq (3.32)	125
5.26	Thermal diffusivity versus temperature from 100 to 300K for $(\text{La}_{1-x}\text{Er}_x)_{0.67}\text{Ca}_{0.33}\text{MnO}_3$ [$0 \leq x \leq 0.03$]	126
5.27	Thermal wave response from CNTs samples at room temperature fitted with theoretical model based on Eq (3.32).	128

5.28	Thermal diffusivity versus percentage of CNTs at room temperature	129
5.29	Thermal diffusivity of the samples at temperatures versus CNTs composition at respective measurement temperature.	130
5.30	Thermal wave response from Emeraldine Base (EB) and Emeraldine Salt (ES) samples at room temperature fitted by theoretical model based on Eq (3.32).	131
5.31	Thermal diffusivity versus temperature from 100 to 300K for Emeraldine Base (EB) and Emeraldine Salt (ES)	132
5.32	Thermal wave response for $\text{Ni}_{0.3}\text{Cu}_{0.2}\text{Zn}_{0.5}\text{Fe}_2\text{O}_4$ and $\text{Ni}_{0.3}\text{Cu}_{0.1}\text{Zn}_{0.6}\text{Fe}_2\text{O}_4$ at room temperature fitted by theoretical model based on Eq (3.32).	133
5.33	Thermal diffusivity versus porosity for $\text{Ni}_{0.3}\text{Cu}_{0.2}\text{Zn}_{0.5}\text{Fe}_2\text{O}_4$ and $\text{Ni}_{0.3}\text{Cu}_{0.1}\text{Zn}_{0.6}\text{Fe}_2\text{O}_4$	134
5.34	Schematic diagram of the physical picture of a porous sample, where the arrows inside show the heat flow, the dark regions are the solid phases and the empty regions are the pore spaces.	135

LIST OF ABBREVIATIONS

EB	Emeraldine Base
EI	Electron
Er	Erbium
ES	Emeraldine Salt
Fe	Iron
FM	Ferromagnetic Metal
I	Insulator
IR	Infra Red
La	Lanthanum
latt	Lattice
LCMO	La-Ca-Mn-O system
M	Metal
Mn	Manganese
N.A	Normalized Amplitude
Ni	Nickel
O	Oxygen
OPC	Open Photoacoustic Cell
OTTER	Optothermal Transient Emission Radiometry
PD	Photodeflection technique
P ² E	Photopyroelectric effect
PA	Photoacoustic
PM	Paramagnetic

PVDF	Polyvinlidene Difluoride
SEM	Scanning Electron Microscopy
SiC	Silicon Carbide
Sm	Samarium
Sr	Strontium
TC	Temperature Controller
Y	Yttrium
YBCO	Y-Ba-Cu-O system
Zn	Zinc
AFM	Antiferromagnetic
B ₄ C	Boron Carbide
Ba	Barium
BCS theory	Bardeen, Cooper and Schrieffer theory
Bi	Bismuth
BSCCO	Bi-Sr-Ca-Cu-O system
C	Carbon
Ca	Calcium
CMR	Colossal Magnetoresistance
CNTs	Carbon Nanotubes
CPC	Closed Photoacoustic Cell
Cu	Copper
Cu	Copper
CW	Continues wave

LIST OF SYMBOLS

t_c	Characteristic rise time of the rear face temperature
θ	Debye temperature of the lattice
ρ	Density
ϵ	Dielectric constant
δ	Dirac symbol
ϵ	Emissivity of the surface
E_0	Energy/unit area absorbed in the material
\bar{q}	Heat flow
Q	Heat pulse energy
θ_0	Initial temperature rise at the surface
$\beta(\lambda)$	Optical absorption coefficient
$A(\lambda)$	Optical absorption length
l_{Phonon}	Phonon free path
v_{Phonon}	Phonon velocity
τ	Pulse time duration
σ	Stefan's constant
$\vec{\nabla}T$	Temperature gradient
ℓ	The distance, where temperature reaches to maximum at a time ξ after the excitation
α	Thermal diffusivity
ξ	Thermal transit time